ELSEVIER

11 January 1996

PHYSICS LETTERS B

Physics Letters B 366 (1996) 56–62

Antibaryon production in sulphur-nucleus collisions at 200 GeV per nucleon

NA35 Collaboration

T. Alber[i], H. Appelshäuser[f], J. Bächler[e], J. Bartke[d], H. Białkowska[ℓ], M.A. Bloomer[c], R. Bock[e], W.J. Braithwaite[j], D. Brinkmann[f], R. Brockmann[e], P. Bunčić[e], P. Chan[j], J.G. Cramer[j], P.B. Cramer[j], I. Derado[i], V. Eckardt[i], J. Eschke[f], C. Favuzzi[b], D. Ferenc[m], B. Fleischmann[e], P. Foka[e], P. Freund[i], M. Fuchs[f], M. Gaździcki[f], E. Gładysz[d], J. Grebieszkow[k], J. Günther[f], J.W. Harris[c], M. Hoffmann[g], P. Jacobs[c], S. Kabana[f], K. Kadija[i,m], M. Kowalski[d], A. Kühmichel[f], J.Y. Lee[f], A. Ljubičić jr.[m], S. Margetis[c], J.T. Mitchell[c,1], R. Morse[c], E. Nappi[b], G. Odyniec[c], G. Paić[m], A.D. Panagiotou[a], A. Petridis[a], A. Piper[h], F. Posa[b], A.M. Poskanzer[c], F. Pühlhofer[h], W. Rauch[i], R. Renfordt[f], W. Retyk[k], D. Röhrich[f], G. Roland[f], H. Rothard[f], K. Runge[g], A. Sandoval[e], N. Schmitz[i], E. Schmoetten[g], R. Sendelbach[f], P. Seyboth[i], J. Seyerlein[i], E. Skrzypczak[k], P. Spinelli[b], R. Stock[f], H. Ströbele[f], T.A. Trainor[j], G. Vasileiadis[a], M. Vassiliou[a], D. Vranic[m], S. Wenig[f], B. Wosiek[i,d], X. Zhu[j]

[a] *Department of Physics, University of Athens, Athens, Greece*
[b] *Dipartimento di Fisica, Università di Bari and INFN Bari, Bari, Italy*
[c] *Lawrence Berkeley Laboratory, Berkeley, CA, USA*
[d] *Institute of Nuclear Physics, Cracow, Poland*
[e] *Gesellschaft für Schwerionenforschung (GSI), Darmstadt, Federal Republic of Germany*
[f] *Fachbereich Physik der Universität, Frankfurt, Federal Republic of Germany*
[g] *Fakultät für Physik der Universität, Freiburg, Federal Republic of Germany*
[h] *Fachbereich Physik der Universität, Marburg, Federal Republic of Germany*
[i] *Max-Planck-Institut für Physik, München, Federal Republic of Germany*
[j] *University of Washington, Seattle, USA*
[k] *Institute for Experimental Physics, University of Warsaw, Warsaw, Poland*
[ℓ] *Institute for Nuclear Studies, Warsaw, Poland*
[m] *Rudjer Bošković Institute, Zagreb, Croatia*

Received 7 July 1995; revised manuscript received 25 October 1995
Editor: J.P. Schiffer

Abstract

Antiproton production near midrapidity has been studied in central collisions of ^{32}S with sulphur, silver and gold nuclei at 200 GeV per nucleon. The measured transverse mass distributions can be described by an exponential with inverse slope parameters of about 200 MeV, similar to those obtained from $\bar{\Lambda}$ spectra. The rapidity density increases weakly with the

SSDI 0370-2693(95)01379-2

target mass, ranging from 0.4 to 0.7. The ratio $\overline{\Lambda}/\overline{p}$ near midrapidity is approximately 1.4 on average, significantly larger than the corresponding ratio observed in proton-proton and proton-nucleus collisions.

Information about baryons and mesons in the hadronic final state is important for understanding the reaction dynamics of relativistic heavy ion collisions. In particular, the study of antibaryons, such as $\overline{\Lambda}$ and $\overline{p}$, near midrapidity in central nucleus-nucleus collisions may shed light on the mechanisms of antiquark production. The ratio $\overline{\Lambda}/\overline{p}$ provides information on the production of strange antiquarks compared to light antiquarks. Antibaryon yields in central nucleus-nucleus collisions are expected to exhibit the subtle interplay between various partonic and/or hadronic production and annihilation processes as well as properties of a possible partonic equilibration of the system [1–9]. Theoretical consideration of the possible creation of a quark gluon plasma in ultrarelativistic nuclear collisions [10] has indicated that strange/antistrange quark pairs might be copiously produced, resulting in an approximate flavour symmetry among light quarks, namely up, down and strange [11]. Under such conditions the $\overline{\Lambda}/\overline{p}$-ratio, which roughly reflects the $\overline{s}/\overline{u}$-ratio, should approach unity (or larger for non-zero baryon densities) [11], far exceeding the value of ~ 0.25 observed in proton-proton collisions. In this letter we shall present a detailed study of antibaryon production in central S+S, S+Ag and S+Au collisions and a comparison with models. Since the results on $\overline{\Lambda}$ production in central sulphur-nucleus collisions have been published recently [12], we will focus on $\overline{p}$ production and shall show that the $\overline{\Lambda}/\overline{p}$-ratio assumes values larger than unity in central collisions.

Experiment NA35 at the CERN SPS investigates collisions of ^{32}S-projectiles of 200 GeV per nucleon incident energy with nuclear targets. The main detectors are two large-volume tracking devices: a streamer chamber inside a 1.5 Tesla magnet and a time projection chamber (TPC) positioned in the field-free region downstream from the magnet [12]. Both detectors record the trajectories of charged particles from which the particle momenta are derived. The acceptances of the detectors for negatively charged hadrons are complementary and cover the full phase space with some overlap. Central events are selected by the absence of projectile spectators in a veto calorimeter placed downstream [12–15]. The central collision fractions of the inelastic cross sections of the nucleus-nucleus collisions, on which we are focusing, are 3%, 3.2% and 6% for the S+S, S+Ag and S+Au collisions, respectively.

The objective of the experiment is to measure the hadronic final state in nucleus-nucleus collisions. In addition to negatively and positively charged particles, weak decays of charged and neutral particles can be detected in the streamer chamber. The TPC on the other hand identifies charged particles by multiple sampling of the specific ionisation with a dE/dx resolution of about 5–6% in the momentum range of the relativistic rise, where particle identification using statistical methods is possible. Combining both detectors, spectra of negative hadrons, net protons ($p - \overline{p}$), K^0_S, K^+, K^-, Λ, $\overline{\Lambda}$ and $\overline{p}$ are obtained. Simulations based on the measured $\overline{\Lambda}$ production show that typically 25–30% of all detected $\overline{p}$ stem from $\overline{\Lambda}$ decays. The measurement of $\overline{\Lambda}$ and $\overline{p}$ in the same experiment is essential for a model-independent correction of this contamination in the $\overline{p}$ spectra.

The TPC covers one unit in rapidity ($3 \leq y \leq 4$) and the entire range of transverse momenta ($0 \leq p_T \leq 2$ GeV/c) for antiprotons. The $\overline{p}$ are separated from kaons and pions by a statistical method based on multiple measurements of the specific ionisation of charged particles traversing the TPC. Sampling the ionisation up to 60 times per reconstructed track results in a Landau-distributed energy-loss spectrum. Applying the *truncated mean* method by ordering the energy losses and discarding the highest values up to 30% (which originate from highly energetic δ-electrons), leads to a gaussian-distributed spectrum of the mean energy loss dE/dx for particles with a fixed momentum [16,17]. The relative dE/dx resolution achieved is 4% for deuteron beam tracks and 5.9–6.4% in the case of high multiplicity events in which the number of usable samples per track – and thus the resolution – are reduced due to the high track density [18].

[1] Now at Brookhaven National Laboratory, Upton, NY, USA.

Particle identification based on the specific ionisation requires an accurate determination of the particle momentum. Track reconstruction in the NA35 TPC provides correct momentum information for primary tracks emerging from the production vertex, but not for secondary tracks – primarily weak decay products and tracks from interactions of produced particles in the detector materials. The main contribution of this background results from decays of Λ, $\overline{\Lambda}$ and K^0_S. Since many of these decays occur between the target and the TPC, charged decay products such as p, $\overline{p}$ and $\pi^{\pm}$ are not deflected by the full magnetic field. As a result a momentum determination based on a straight line trajectory in the TPC outside the magnet overestimates the momentum. In order to correct for the corresponding distortion of the dE/dx spectra, strange particles were generated with a phase space population determined by the measured distributions [19]. These particles were passed to a GEANT simulation package [20] implemented with the NA35 detector geometry. Raw data were then generated using a detector response simulator and analyzed in the same way as real data. The simulated dE/dx distribution of the decay products accepted by the TPC track reconstruction program is finally subtracted from the measured dE/dx distribution.

The dE/dx resolution achieved is approximately 6%. This results in a 1–2 standard deviation separation between $\overline{p}$ and K^-, and up to 2.5 standard deviations in the case of K^- and π^- in the relativistic rise. In order to obtain spectra for various particle species a statistical method of particle identification must be applied to the data. A gaussian distribution of the energy loss of each particle type ($\overline{p}$, K^-, π^-, e^-) for a given momentum is assumed, implying that a superposition of four gaussian distributions describes the dE/dx spectrum in any given range of momentum. A Monte Carlo study has demonstrated the validity of the deconvolution method using gaussian distributions to fit in (y, p_T) bins.

To deconvolute the dE/dx distribution, the data are parametrized in small p_T (0.2 GeV/c) intervals in a given y range by the function

$$f(dE/dx \mid \Phi_i) = \sum_i \Phi_i \exp\left(-\frac{(dE/dx - \mu_i)^2}{2\cdot(\sigma\cdot\mu_i)^2}\right), \quad i = \overline{p}, K^-, \pi^-, e^-, \tag{1}$$

where the fitted parameters Φ_i are proportional to the particle yields, μ_i is the mean dE/dx of a particle in a given (y, p_T) bin and σ is the relative width of the dE/dx distribution. The μ_i are calculated from a parametrisation of the relativistic rise [21] adapted to NA35 data by using identified pions, electrons and protons, whereas σ is the relative resolution achieved in high multiplicity events.

The extracted particle yields, especially the kaon yield, depend crucially on the dE/dx resolution achieved, which itself varies with the track density of the TPC event. Therefore a careful determination of the relative dE/dx resolution for each target-projectile system is necessary. The relative dE/dx resolution σ is 5.9, 6.1 and 6.4% for the S+S, S+Ag and S+Au systems, respectively.

An analysis of the systematic errors exhibits a sensitivity of the fit to the uncertainties of the parameters μ_i and σ of the order of 5–15% for antiprotons. A comparison of the kaon yields extracted from the above dE/dx analysis to results obtained by analysis of the $K^{\pm}$ kink-decay topology allows for another independent estimate of possible systematic errors. The decays of charged kaons have been measured both in the NA35 streamer chamber and in the TPC [12,22,23]. The results on K^- yields obtained by both methods agree within 25%, i.e. within the errors [18]. Fixing the K^- yield to the value determined from the kink analysis gives another handle on the antiproton systematic error and results in a 15–20% change in the antiproton yields. All the above studies allow us to estimate the total systematic error in the antiproton yields to be 20–25%, which includes the uncertainties of the deconvolution and the error of the background subtraction (typically 5%). These errors are included in the quoted errors of $\overline{p}$ spectra.

Fig. 1 (top) shows the background corrected dE/dx distribution of particles produced in central S+Au collisions at 200 GeV per nucleon in a $y - p_T$ bin (the antiproton mass was assumed for all particles in the rapidity calculation) of $3 \leq y \leq 4$ and $0.8 \leq p_T \leq 1.2$ GeV/c together with the fit result. The fit describes the spectrum well, even though it deviates from the spectrum in the dE/dx range between kaons and pions due to the sensitivity to the resolution discussed above and the uncertainty in the corrections. Fig. 1 (bottom) shows the four gaussian distributions obtained from the fitted parameters Φ_i and the appropriate values

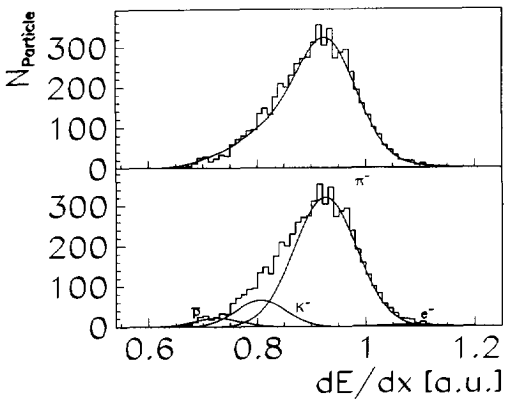

Fig. 1. The dE/dx spectrum of negatively charged particles produced in central S+Au data at 200 GeV per nucleon together with the fitted curve (top) and its decomposition into single particle contributions (bottom) in the p_T interval from 0.8 to 1.2 GeV/c and the rapidity interval from 3 to 4 (the antiproton mass is assumed for all particles).

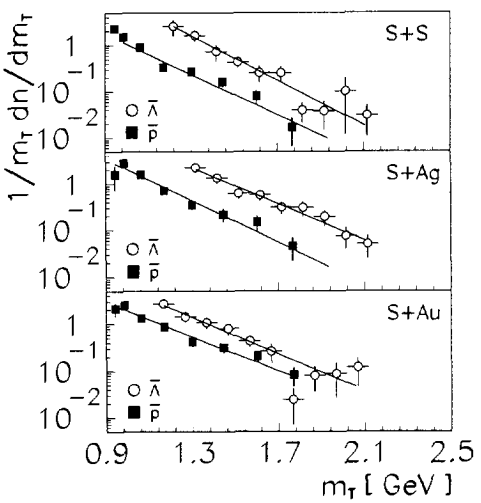

Fig. 2. Transverse mass distributions of $\overline{p}$ ($3 \leq y \leq 4$) and $\overline{\Lambda}$ (S+S, S+Ag at $1 \leq y \leq 3$, S+Au at $3 \leq y \leq 5$) produced in central sulphur-nucleus collisions at 200 GeV per nucleon. The solid lines are exponential fits (see Eq. (2)). The vertical scale is in GeV^{-2}.

of μ_i and σ. The extracted yields are then corrected for geometrical acceptance, tracking inefficiency and quality cuts in order to obtain cross sections.

The invariant spectra of the antibaryons, $\overline{p}$ and $\overline{\Lambda}$, as a function of the transverse mass m_T are shown in Fig. 2. The distributions are compatible with an exponential

$$\frac{1}{m_T}\frac{dn}{dm_T} = C \cdot \exp\left(-\frac{m_T}{\mathcal{T}}\right), \tag{2}$$

where C is a normalization factor and $\mathcal{T}$ is the inverse slope parameter. These two parameters are determined by fitting the experimental data. The inverse slope parameters are around 200 MeV and show a slight target mass dependence (see Table 1). Experiment NA44 has reported similar inverse slope parameters for antiprotons near midrapidity ($\mathcal{T} = 175 \pm 6$ MeV for central S+S and $\mathcal{T} = 215 \pm 6$ MeV for S+Pb collisions at 200 GeV per nucleon) [24].

The rapidity densities of $\overline{p}$ and $\overline{\Lambda}$ at ($3 \leq y \leq 4$) for central sulphur-nucleus collisions are given in Table 2. The extrapolation of the measured particle yields into the m_T regions outside the acceptance was based on the exponential m_T parametrization (see Eq. (2)). The rapidity density of $\overline{\Lambda}$s produced in S+Ag collisions in the $\overline{p}$ acceptance is obtained from averaging S+S and S+Au data. Because these data cover the acceptance completely and since no target dependence is observed at rapidities above midrapidity, the systematic uncertainty of this procedure is expected to be small. The yields contain primordial $\overline{\Lambda}$ as well as $\overline{\Lambda}$ from decays of heavier antihyperons (contributing typically about 30%) [12]. There seems to be a weak increase in the $\overline{p}$ yield with increasing target mass, whereas the $\overline{\Lambda}$ yield in the rapidity interval studied is independent of the target mass number.

In order to compare the results of this experiment with preliminary data from the NA44 experiment, all $\overline{p}$ from $\overline{\Lambda}$ decays have been added to the primordial yields, resulting in a rapidity density for central S+S collisions of 0.9 ± 0.1 and for central S+Au collisions of 1.2 ± 0.2. A similar trend in the target mass dependence is seen in preliminary NA44 data for $\overline{p}$ produced at $y = 2.8$ in central S+S ($dn/dy = 0.4 \pm 0.1$ [24]) and S+Pb collisions ($dn/dy = 1.4 \pm 0.2$ [24]), but the yields are different.

Since $\overline{\Lambda}$ and $\overline{p}$ data at midrapidity in minimum bias proton-proton, proton-neutron and minimum bias proton-nucleus collisions are sparse, results from various experiments must be compiled, analysed [12,25,26,28–31] and compared (see Table 2 for the results). When necessary, particle yields have been extrapolated into the m_T regions outside the acceptance assuming an exponential m_T or p_T distribution. The ISR data cover a wide m_T-range at midrapidity

Table 1
Inverse slope parameters T for $\overline{p}$ and $\overline{\Lambda}$ produced in central S+S, S+Ag and S+Au collisions at 200 GeV per nucleon. The errors include systematic uncertainties

Reaction	$\overline{p}$		$\overline{\Lambda}$	
	rapidity interval	inverse slope parameter T	rapidity interval	inverse slope parameter T
S+S	$3 \leq y \leq 4$	184 ± 14 MeV	$1 \leq y \leq 3$	180 ± 24 MeV
S+Ag	$3 \leq y \leq 4$	189 ± 15 MeV	$1 \leq y \leq 3$	221 ± 24 MeV
S+Au	$3 \leq y \leq 4$	239 ± 20 MeV	$3 \leq y \leq 5$	223 ± 22 MeV

Table 2
Rapidity densities of $\overline{p}$, $\overline{\Lambda}$ and h^- produced in central sulphur-nucleus collisions at $3 \leq y \leq 4$ and minimum bias nucleon-nucleon and proton-nucleus interactions at $y = 3$ [a,b]. The value of the $\overline{\Lambda}$ rapidity density for S+Ag collision is not directly measured, but estimated as the average of the corresponding values for S+S and S+Au collisions (see text). This number and the ratio $\overline{\Lambda}/\overline{p}$ are therefore shown in italics

Reaction	$\frac{dn}{dy}(\overline{p})$	$\frac{dn}{dy}(\overline{\Lambda})$	$\overline{\Lambda}/\overline{p}$	$\frac{dn}{dy}(h^-)$
S+S	0.4 ± 0.1	0.75 ± 0.16	$1.9\ ^{+0.7}_{-0.6}$	25 ± 1
S+Ag	0.6 ± 0.2	*0.75 ± 0.19*	*1.3* $^{+0.7}_{-0.5}$	40 ± 2
S+Au	0.7 ± 0.2	0.75 ± 0.10	$1.1\ ^{+0.4}_{-0.3}$	47 ± 5
N+N	$(2.0 \pm 0.2) \cdot 10^{-2}$	$(0.5 \pm 0.2) \cdot 10^{-2}$	0.25 ± 0.10	0.74 ± 0.04
p+S	$(3.2 \pm 0.3) \cdot 10^{-2}$		0.5 ± 0.1	1.3 ± 0.2 [27]
		$(1.5 \pm 0.3) \cdot 10^{-2}$		[25]
		$(2.05 \pm 0.25) \cdot 10^{-2}$		[12]
p+Au	$(4.6 \pm 0.5) \cdot 10^{-2}$	$(1.5 \pm 0.5) \cdot 10^{-2}$	0.3 ± 0.1	1.6 ± 0.1

[a] The rapidity density of $\overline{\Lambda}$ for the Ag target was interpolated between the data from the S and Au target [12]. The $\overline{\Lambda}$ data from p+S collisions [12,25] have to be corrected for a trigger bias ($h^{+/-} \geq 5$). The p+S data set [25] and the $\overline{\Lambda}$ for p+Au collisions [26] do not contain the feed-downs from antihyperon decays. The corrected $\overline{\Lambda}$ yield at midrapidity for minimum bias p+S collisions (data set [27]) is $(1.5 \pm 0.3) \cdot 10^{-2}$.

[b] The h^- rapidity density for p+S collisions [34] had to be corrected for a trigger bias ($h^{+/-} > 5$). This correction was based on the measured total h^- multiplicities for the various p+S data sets [12,25].

but were taken at higher $\sqrt{s} = 23$ GeV. The Fermilab data on $\overline{p}$ production in p+p and p+A collisions were taken at 200 GeV/c ($\sqrt{s} = 19.4$ GeV), but cover only high p_T. Combining both data sets one finds that the $\overline{p}$ production at midrapidity in p+p collisions increases by about 15% from $\sqrt{s} = 20$ GeV to 23 GeV [32,33].

The ratio $\overline{\Lambda}/\overline{p}$ is expected to be a good measure of strange quark production as compared to the production of non-strange quarks, because the valence antiquark content of the $\overline{\Lambda}$ is $\overline{u}\overline{d}\overline{s}$ and that of the $\overline{p}$ is $\overline{u}\overline{d}\overline{u}$. This ratio reflects the yield of $\overline{s}$-quarks relative to that of non-strange light quarks $\overline{q}$. Furthermore, the antiquarks of these antibaryons are newly created so that their distributions should not directly reflect the distributions of the valence quarks of the incoming nuclei. However, since antibaryons have a large annihilation cross section with nucleons which are abundant in the central rapidity region [35,36], the antibaryon yields in central nucleus-nucleus collisions should be sensitive to the net baryon density.

These concepts make the $\overline{\Lambda}/\overline{p}$-ratio a valuable tool for studying quark/hadron production in a baryon-rich environment. One expects a dramatic increase in this ratio when going from minimum bias p+p collisions, in an almost baryon-free midrapidity region with strangeness suppression, to central sulphur-nucleus collisions where high baryon densities and reduction of strangeness suppression are observed at midrapidity [12,36]. The $\overline{\Lambda}/\overline{p}$-ratio near midrapidity in proton-proton, minimum bias proton-nucleus and central nucleus-nucleus collisions is shown in Fig. 3 as a function of the rapidity density at midrapidity of neg-

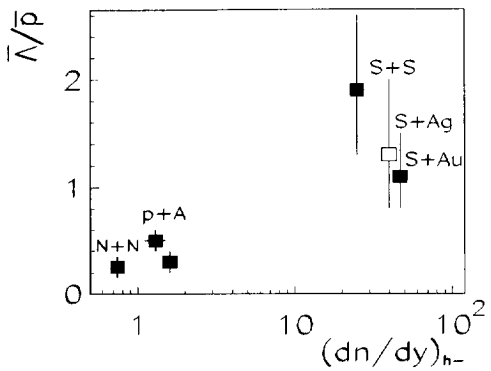

Fig. 3. $\overline{\Lambda}/\overline{p}$-ratio near midrapidity in proton-proton, minimum bias proton-nucleus and central nucleus-nucleus collisions at 200 GeV per nucleon as a function of the rapidity density of negatively charged hadrons at midrapidity. The result for S+Ag (open symbol) is not the result of a direct measurement (see text).

Table 3
Ratio of rapidity densities of $\overline{\Lambda}$ and $\overline{p}$ in the rapidity interval $3 \leq y \leq 4$ (RQMD) and in full phase space (generalized thermal approach [9,39,40]). For both models $\overline{\Lambda}$s contain feed-downs from $\overline{\Xi}$ and $\overline{p}$ do not contain $\overline{p}$ from $\overline{\Lambda}$ decays as in the case of the experimental data

Reaction	RQMD 1.08			Generalized thermal approach
	$\frac{dn}{dy}(\overline{p})$	$\frac{dn}{dy}(\overline{\Lambda})$	$\overline{\Lambda}/\overline{p}$	$\overline{\Lambda}/\overline{p}$
p+p	$1.5 \cdot 10^{-2}$	$0.5 \cdot 10^{-2}$	0.3	0.2
S+S	0.7	0.75	1.1	1.5
S+Ag	1.0	0.9	0.9	-
S+Au/Pb	1.4	1.2	0.9	1.1

atively charged hadrons h^-. The ratio increases from a value of 0.25 for p+p (and p+A) collisions to a value of approximately 1.4 for central S+A collisions (subtracting the feed-downs from decays of heavier antihyperons into $\overline{\Lambda}$ – typically 30% – would give a ratio at freeze-out of about 1 for the nucleus-nucleus reactions). The increase in the ratio can be studied in more detail for the S+S system. If rapidity densities at midrapidity in nucleon-nucleon collisions are scaled by the ratio of h^--multiplicities in central S+S and in nucleon-nucleon collisions (see Table 2), the $\overline{p}$ production decreases by about 30 % and the $\overline{\Lambda}$ abundance at midrapidity is strongly enhanced by a factor of 5.

Models of nucleus-nucleus collisions assuming independent superpositions of nucleon-nucleon-like interactions (e.g. FRITIOF [37]) predict no change of the $\overline{\Lambda}/\overline{p}$-ratio when going from p+p to central nucleus-nucleus collisions. Therefore, inclusion of secondary processes at a partonic and/or hadronic level is needed to explain the data. The string-hadronic RQMD model including secondary collisions underestimates the $\overline{\Lambda}$ production in central S+S collisions at 200 GeV per nucleon by a factor of 5 and the $\overline{p}$ yield by a factor of about 3 [1]. By adding a new reaction mechanism (RQMD 1.08), namely the fusion of strings into color ropes in the early stage of the reaction, the model reproduces the measured rapidity distributions of $\overline{\Lambda}$ by means of enhanced production of antibaryons, although for the antiprotons this increase is partially compensated by their large absorption. The prediction of the model, however, exceeds the actual $\overline{p}$ yield by 75%. Therefore the $\overline{\Lambda}/\overline{p}$-ratio predicted by RQMD is lower than the measured value. The predictions for central S+Ag and S+Au collisions for this ratio are close to 1, but the model overestimates the $\overline{\Lambda}$ and $\overline{p}$ yields (see Table 3) [38]. Attempts to describe the antibaryon yields within the RQMD model require the introduction of a new production mechanism beyond hadronic rescattering.

Thermal models assume that hadrons freeze-out in chemical equilibrium. The generalised thermal approach [9,39], excluding pions from the chemical analysis and allowing only partial equilibration of strangeness, reproduces $\overline{\Lambda}$ and $\overline{p}$ yields and consequently the $\overline{\Lambda}/\overline{p}$-ratio (see Table 3). The fitted strangeness saturation factor for central S+S collisions [39] is close to unity (about 0.9 for S+Au collisions [40]) and the strange chemical potential is close to zero. Both values may be interpreted as a consequence of the formation of the deconfined phase at the early stage of the collision.

In summary, experiment NA35 at CERN has measured $\overline{\Lambda}$ and $\overline{p}$ production near midrapidity in central S+S, S+Ag and S+Au collisions. The inverse slope values of the m_T-spectra of these antibaryons are all about 200 MeV. The measured ratio $\overline{\Lambda}/\overline{p}$ of approximately 1.4 near midrapidity is significantly larger than the ratio measured in p+p interactions and minimum bias p+A collisions and shows a slight tendency to decrease with the target mass in sulphur-nucleus collisions.

Acknowledgements

This work was supported by the Bundesministerium für Forschung und Technologie and by the Leibniz Grant of the Deutsche Forschungsgemeinschaft, Germany, by the US Department of Energy (DE–AC03–76SF00098), by the Polish State Committee for Scientific Research (204369101), by the Polish-German Foundation (565/93) and by the Commission of European Communities (CI-0250YU(A)).

References

[1] H. Sorge et al., Phys. Lett. B 289 (1992) 6.
[2] A. Jahns et al., Phys. Rev. Lett. 68 (1992) 2895.
[3] A. Jahns et al., Phys. Lett. B 308 (1993) 11; B 314 (1993) 482(E), 483(E).
[4] S. Gavin et al., Phys. Lett. B 234 (1990) 175.
[5] S.H. Kahana et al., Phys. Rev. C 47 (1993) R1356.
[6] K. Werner, Phys. Rep. 232 (1993) 87.
[7] J. Rafelski, Phys. Lett. B 262 (1991) 333.
[8] J. Letessier et al., Phys. Lett. B 292 (1992) 417.
[9] J. Letessier et al., Phys. Rev. D 51 (1995) 3408.
[10] E.V. Shuryak, Phys. Rep. 61 (1980) 71; 115 (1984) 151.
[11] P. Koch et al., Phys. Rep. 142 (1986) 167.
[12] T. Alber et al., Z. Phys. C 64 (1994) 195.
[13] J. Bächler et al., NA35 Collaboration, Z. Phys. C 52 (1991) 239.
[14] J. Bächler et al., NA35 Collaboration, Phys. Rev. Lett. 72 (1994) 1419.
[15] D. Brinkmann et al., Nucl. Instr. Meth. A 354 (1995) 419.
[16] J. Günther, IKF report, IKF-HENPG/8-94 (1994), unpublished.
[17] A.H. Walenta et al., Nucl. Instr. Meth. 161 (1979) 45.
[18] J. Günther and D. Röhrich, IKF report, IKF-HENPG/6-94 (1994), unpublished.
[19] D. Brinkmann, PhD thesis, Univ. of Frankfurt (1995), unpublished.
[20] R. Brun et al., GEANT3 User Guide CERN/DD/EE/84-1 (1986).
[21] R.M. Sternheimer, Phys. Rev. 88 (1952) 851.
[22] J. Bächler et al., NA35 Collaboration, Z. Phys. C 58 (1993) 367.
[23] S. Margetis, LBL report 37085 (1995), unpublished.
[24] J. Dodd, NA44 Collaboration, 11th Int. Conf. on Ultra-Relativistic Nucleus-Nucleus Collisions (Quark Matter 1995), Monterey, California, USA.
[25] J. Bartke et al., NA35 Collaboration, Z. Phys. C 48 (1990) 191.
[26] A. Bamberger et al., NA35 Collaboration, Z. Phys. C 43 (1989) 25.
[27] J. Bächler et al., NA35 Collaboration, Z. Phys. C 51 (1991) 157.
[28] M. Gaździcki und O. Hansen, Nucl. Phys. A 528 (1991) 754.
[29] B. Alper et al., Nucl. Phys. B 100 (1975) 237.
[30] K. Guettler et al., Nucl. Phys. B 116 (1976) 77.
[31] J.W. Cronin et al., Phys. Rev. D 11 (1975) 3105.
[32] A. Wróblewski, in: Proc. Int. Symp. on Multiparticle Dynamics (Kayserberg, 1977) p. A1.
[33] A.M. Rossi et al., Nucl. Phys. B 84 (1975) 269.
[34] D. Röhrich et al., NA35 Collaboration, IKF report, IKF-HENPG/7-94 (1994), to be published.
[35] D. Röhrich, Hadron Production in Nucleus-Nucleus Collisions at SPS- and AGS-Energies, in: Hot and Dense Nuclear Matter, NATO ASI Series B: Physics Vol. 335, ed. by W. Greiner, H. Stöcker and A. Gallmann (Plenum Press, New York and London, 1994) pp. 505.
[36] D. Röhrich et al., Nucl. Phys. A 566 (1994) 35c.
[37] B. Andersson, G. Gustafson and B. Nilsson-Almqvist, Nucl. Phys. B 281 (1987) 289.
[38] H. Sorge, Z. Phys. C 67 (1995) 479.
[39] J. Sollfrank et al., Z. Phys. C 61 (1994) 659.
[40] J. Rafelski et al., in Strangeness and the Search for QGP, ed. by J. Rafelski, (AIP Proceedings Series Volume 330, 1995) p. 490;
J. Letessier et al., to be published.